



3rd International Electronic Conference on Water Sciences



ENERGY DISSIPATION STRUCTURES: INFLUENCE OF AERATION IN SUPERCRITICAL FLOWS

Juan José Rebollo ¹ (juan.j.rebollo@cedex.es)

David López ¹ (david.lopez@cedex.es)

Tamara Ramos ¹ (tamara.ramos@cedex.es)

Luis Garrote ² (l.garrote@upm.es)

¹ Centro de Estudios y Experimentación de Obras Públicas (CEDEX)

² Universidad Politécnica de Madrid (UPM)



MINISTERIO
DE FOMENTO

MINISTERIO
PARA LA TRANSICIÓN ECOLÓGICA

CEDEX
CENTRO DE ESTUDIOS
Y EXPERIMENTACIÓN
DE OBRAS PÚBLICAS



UNIVERSIDAD
POLITÉCNICA
DE MADRID

TABLE OF CONTENTS

1. Experimental facilities

- Physical model
- Supply equipment
- Instrumental devices

2. Influence of aeration in energy dissipation phenomena

3. Experimentation and data collection

4. Test scenarios and results

5. Results analysis and discussion

6. Future activities

7. Conclusions

PHYSICAL MODEL

Experimental facilities: This structure includes all the elements needed to reproduce the scenarios involved in the study. The water entrance is controlled by a open gate with 8 cm high. This section and the air-water flow mixture determine the initial condition of the experiments.

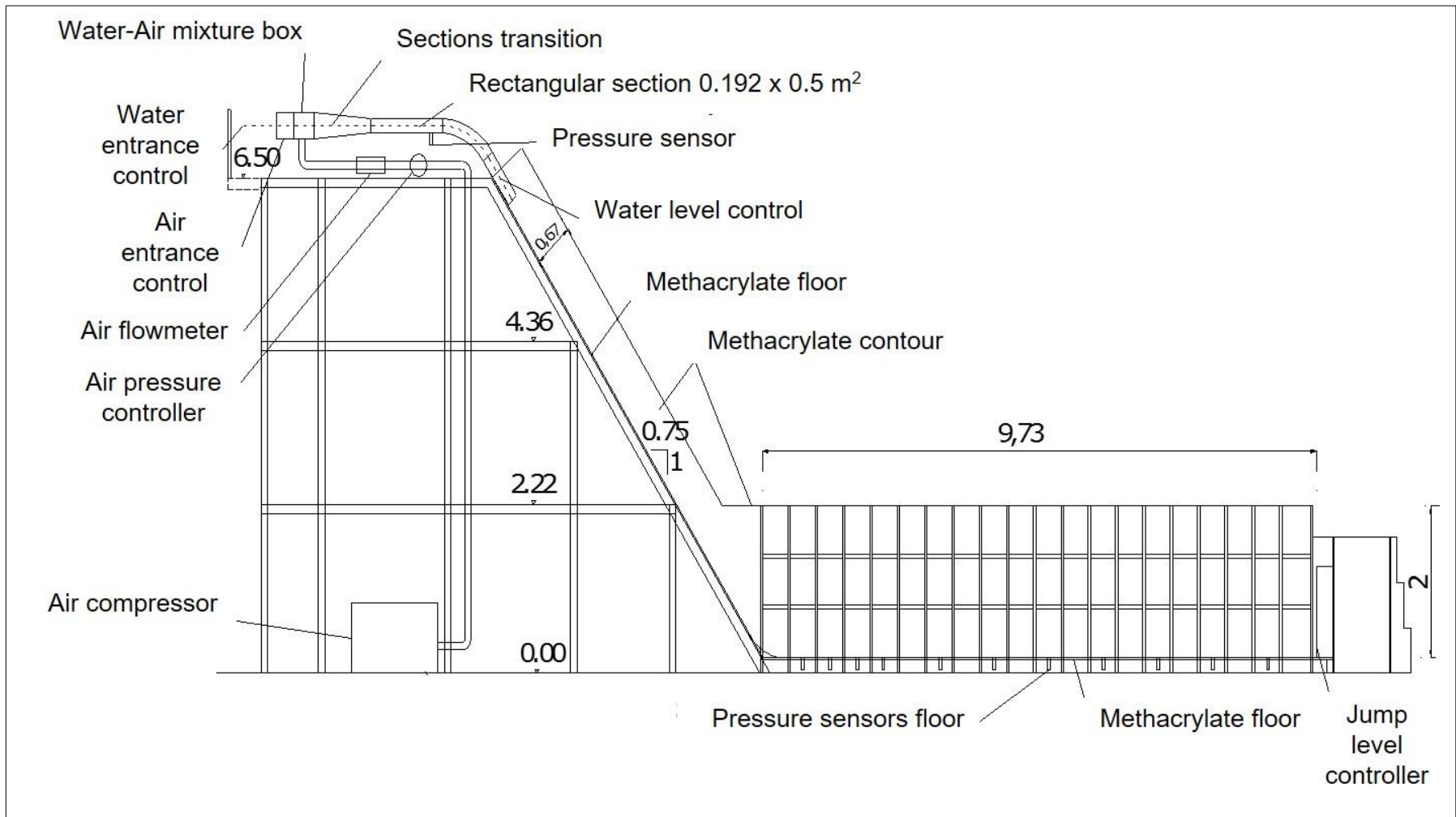


Figure 1. Physical model section

PHYSICAL MODEL

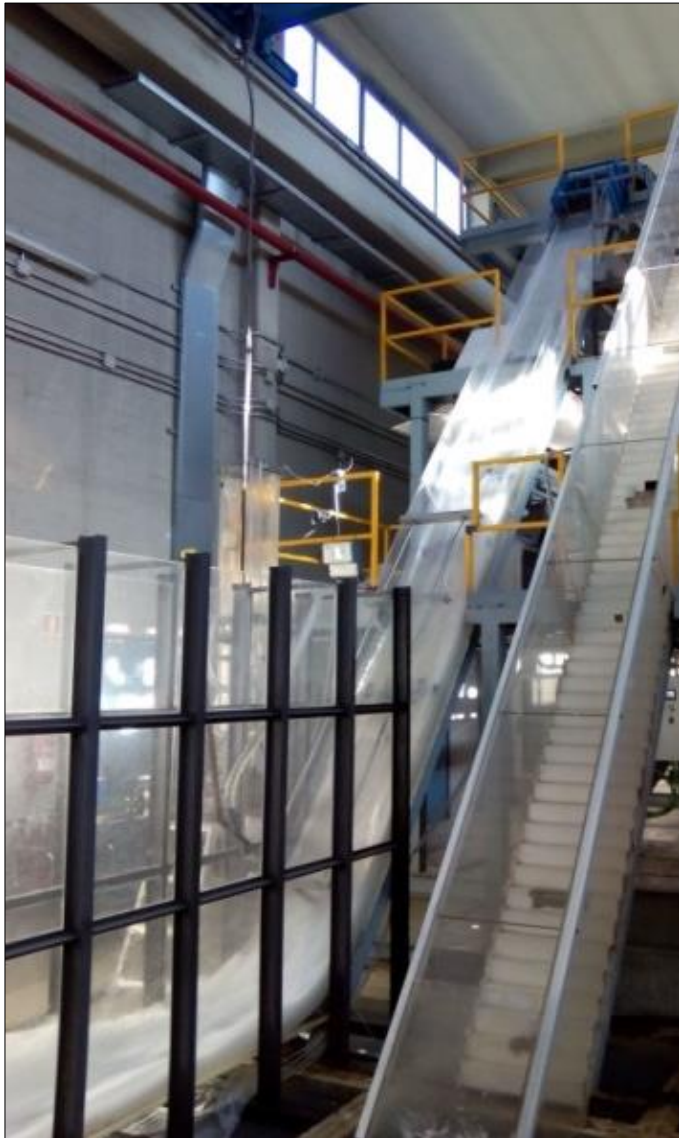


Figure 2. Lateral view of the spillway channel



Figure 3. Global view of physical model with spillway and still basin

PHYSICAL MODEL

Border conditions: Intake flow through section with 0.5 m wide and 0.08 m high (Figure 4) and regulated gate at the final of the still basin to control the hydraulic jump length (Figure 5)



Figure 4. Intake flow section gate

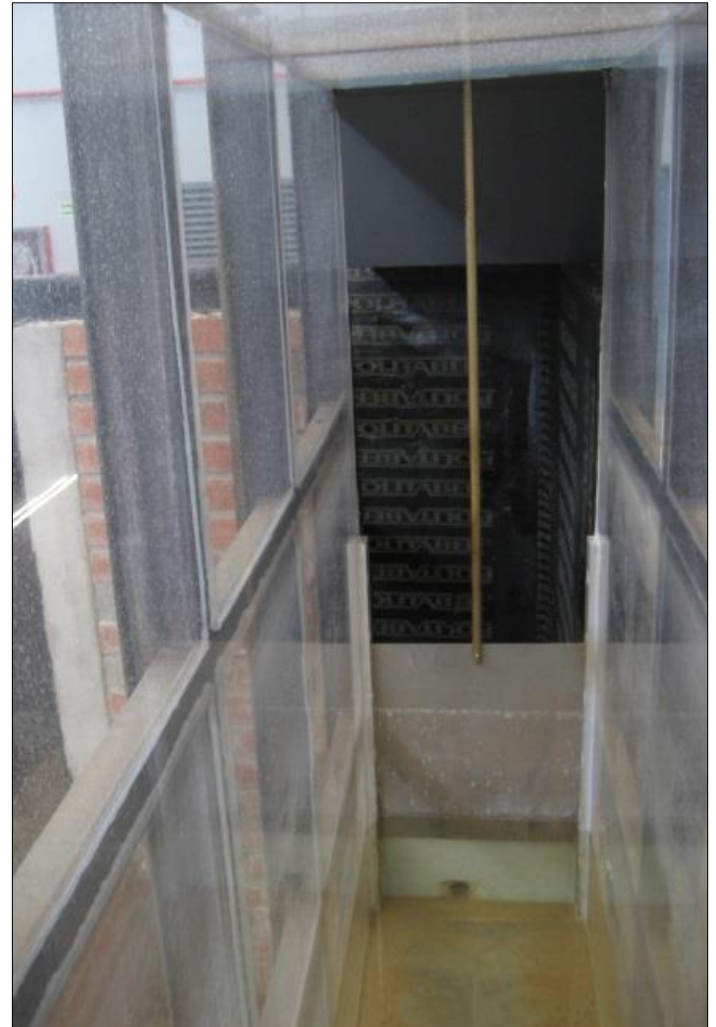


Figure 5. Regulated gate to close the still basin

SUPPLY EQUIPMENT



Figure 6. General water gauger



Figure 7. Water pump



Figure 8. Air compressor



Figure 9. Air – water mixture box

INSTRUMENTAL DEVICES



Figure 10. Water electromagnetic flowmeter



Figure 11. Air flowmeter



Figure 12. Air pressure control

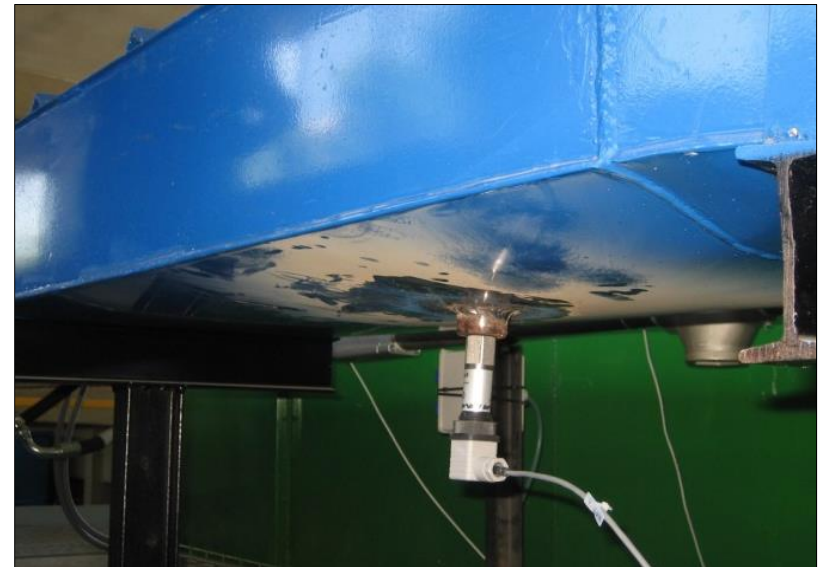


Figure 13. Atmospheric pressure sensor in mixture box

ENERGY DISSIPATION MECHANISMS

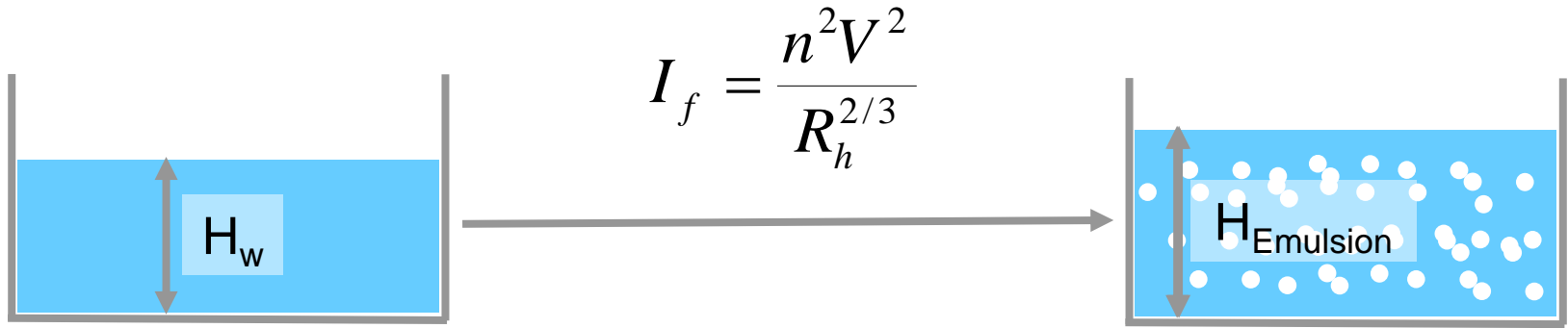
- 1. Contour friction:** The most important effect of energy dissipation in open channel flows → Manning equation (1891) is the most known and widely used in the hydraulic engineering area to determine the friction slope in base to a roughness coefficient n
- 2. Turbulent viscosity:** Hinze (1950) considers that aeration increases the viscosity turbulent dissipation but this formulation is theoretical and without empirical support.
- 3. Bubbles break:** Other authors (Mateos, 1991; Wood, 1991 and Chanson, 1992) consider the division and reunification of bubbles as the main factor over energy losses. In this case, shear stress between flow layers breaks the bubbles to regroup each other's in collision areas later. This process has to exceed the surface tension of the air particles and generates energy dissipation by heat.

Methods 2 and 3 are opposed to the Manning formulation (1) → Both consider the turbulence as main effect of dissipation instead of roughness.

In our experimental case → **Manning formulation is the option to analyze the energy dissipation due to contour friction** is prevailing in supercritical flows with low water depth and high velocity.

The application of other formulations would be interesting during the analysis of the hydraulic jump, where turbulence effects are more important over the flow

CONTOUR FRICTION MECHANISM



I_f : Friction slope / n : Manning roughness coefficient / V : Average velocity / R_h : Hydraulic diameter / H_w : Water Depth / $H_{Emulsion}$: Emulsion Depth

With Q_{water} and n constants \rightarrow Aeration increases $H_{Emulsion}$

For R_h increasing \rightarrow I_f reduction and V increasing

If V increase, with constant Q_w
 H_w decreasing \rightarrow $\tau_b = \gamma_{water} H_w I_f$ \rightarrow τ_b (Bottom stress) decreasing

Aeration reduces the contour friction and this effect generates flow acceleration

2. Influence of aeration in energy dissipation phenomena

FLOW VELOCITY MEASUREMENT

- The flow velocity has been collected by means of a Pitot probe with a pressure sensor and connected to a data acquisition program developed in CEDEX with LabVIEW
- The acquisition frequency is 100 data/s and the recording time achieves 100 s
- Testing point: Final section of the spillway channel
- Results: Average velocity profile with 14 measurement points along the flow height



Figure 14. Velocity measurement testing

AIR CONCENTRATION MEASUREMENT

- Collection of air concentration has carried out with an Air Concentration Meter (ACM) developed by the Hydraulic Engineering Department of the Universidad Politécnica de Cartagena (UPCT)
- This probe is based in a prototype developed by U.S. Department of the Interior Bureau of Reclamation (Jacobs, 1997) to measure the percentage of air entrained in flowing water
- This methodology detects the air bubbles by passing through the water by changes in conductivity that takes place when a bubble impinges on the probe tip
- The acquisition frequency is 60 data/s and the recording time achieves 45 s.
- Testing point: Final section of the spillway channel
- Results: Average air concentration profile with 14 measurement points along the flow height



Figure 15. Air concentration measurement testing

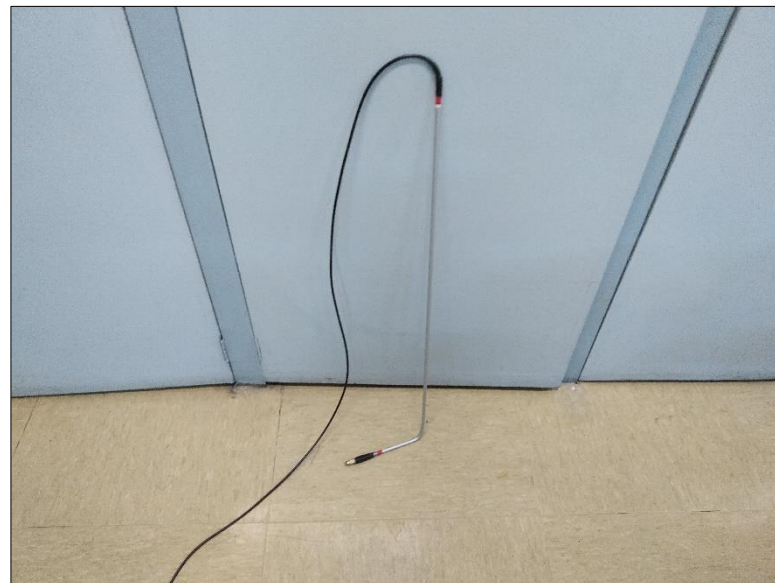


Figure 16. Air concentration meter (ACM) probe

TEST SCENARIOS AND RESULTS AT INTAKE CHANNEL

- Results obtained during the experimental phase → 12 scenarios of air (Q_a) and water (Q_w) flow
- Table 1 shows the average velocity (V_{In}) and air concentration (C_{In}) in the physical model entrance

Scenario	Q_w (m ² /s)	Q_a (l/minute)	V_{In} (m/s)	C_{In} (%)
1.1	0.31 (155 l/s)	0	3.875	0
1.2		1000	4.3045	9.9778
1.3		2000	4.7391	18.2338
2.1	0.4 (200 l/s)	0	5	0
2.2		1000	5.45	8.2569
2.3		2000	5.912	15.4258
3.1	0.5 (250 l/s)	0	6.25	0
3.2		1000	6.7182	6.9692
3.3		2000	7.2063	13.2708
4.1	0.6 (300 l/s)	0	7.5	0
4.2		1000	8.0046	6.3034
4.3		2000	8.5288	12.0631

Table 1. Experimental scenarios tests with average velocity and air concentration at the intake channel

BORDER CONDITION IN SPILLWAY CHANNEL

- To reproduce a real condition of fully turbulent flow, the channel has been covered at the top by a metallic mesh to increase the turbulence along the channel → Flexible material to no hinder free flow (Figure 17)
- A flexible plastic cover has been also disposed over the channel to reduce the air exchange between flow and atmosphere (Figure 18)

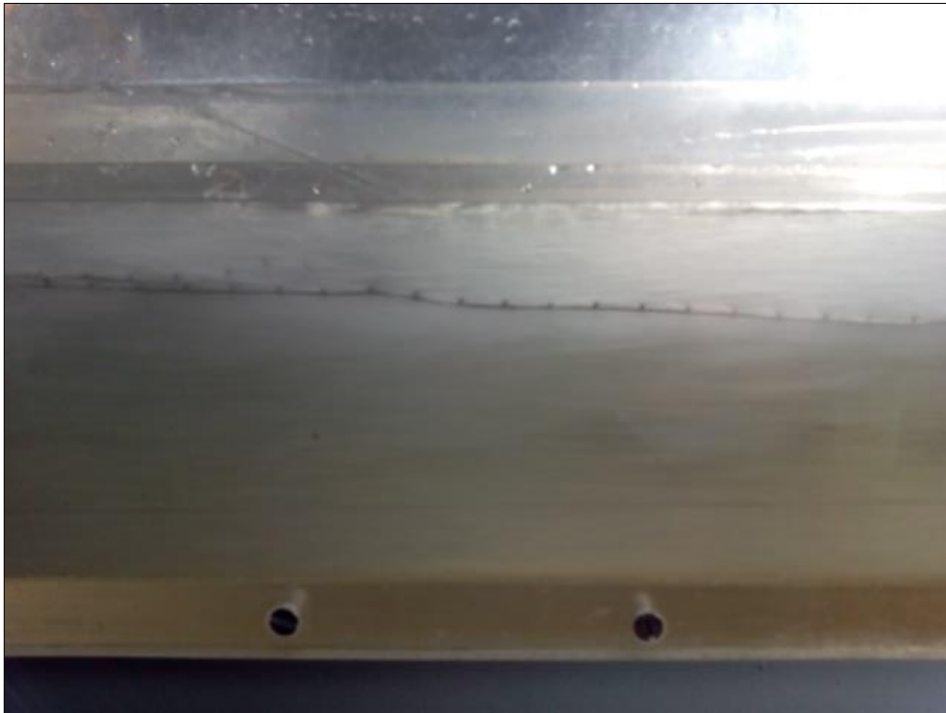


Figure 17. Effects of the metallic mesh and plastic covers over the flow in tests



Figure 18. Border conditions over the flow surface during the experimental analysis

RESULTS AT CHANNEL EXIT SECTION

- Relation between velocity (V_{Out}) and air concentration profiles (C_{Out}) in channel exit section (Table 2)
- Table 2 includes also the depth of the experiments when concentration achieves 90% ($H_{90 Out}$) → very common value considered in the related scientist literature
- Figures 19 – 22 show the elation between velocity and concentration profiles in all scenarios

Scenario	V_{Out} (m/s)	C_{Out} (%)	$H_{90 Out}$ (cm)
1.1	5.1874	29.2792	8.2166
1.2	5.2404	31.2996	8.2375
1.3	5.3541	33.026	8.0971
2.1	5.8814	27.0491	9.075
2.2	5.979	29.5446	9.3555
2.3	6.0255	30.3674	9.5525
3.1	6.3162	23.9025	10.4956
3.2	6.5179	25.7145	10.522
3.3	6.6851	27.8937	10.9652
4.1	6.5939	22.1556	12.2004
4.2	6.8136	22.4595	12.0333
4.3	6.9479	22.8837	12.0434

Table 2. Average velocity, concentration and H90 values at the channel exit

RESULTS AT CHANNEL EXIT SECTION

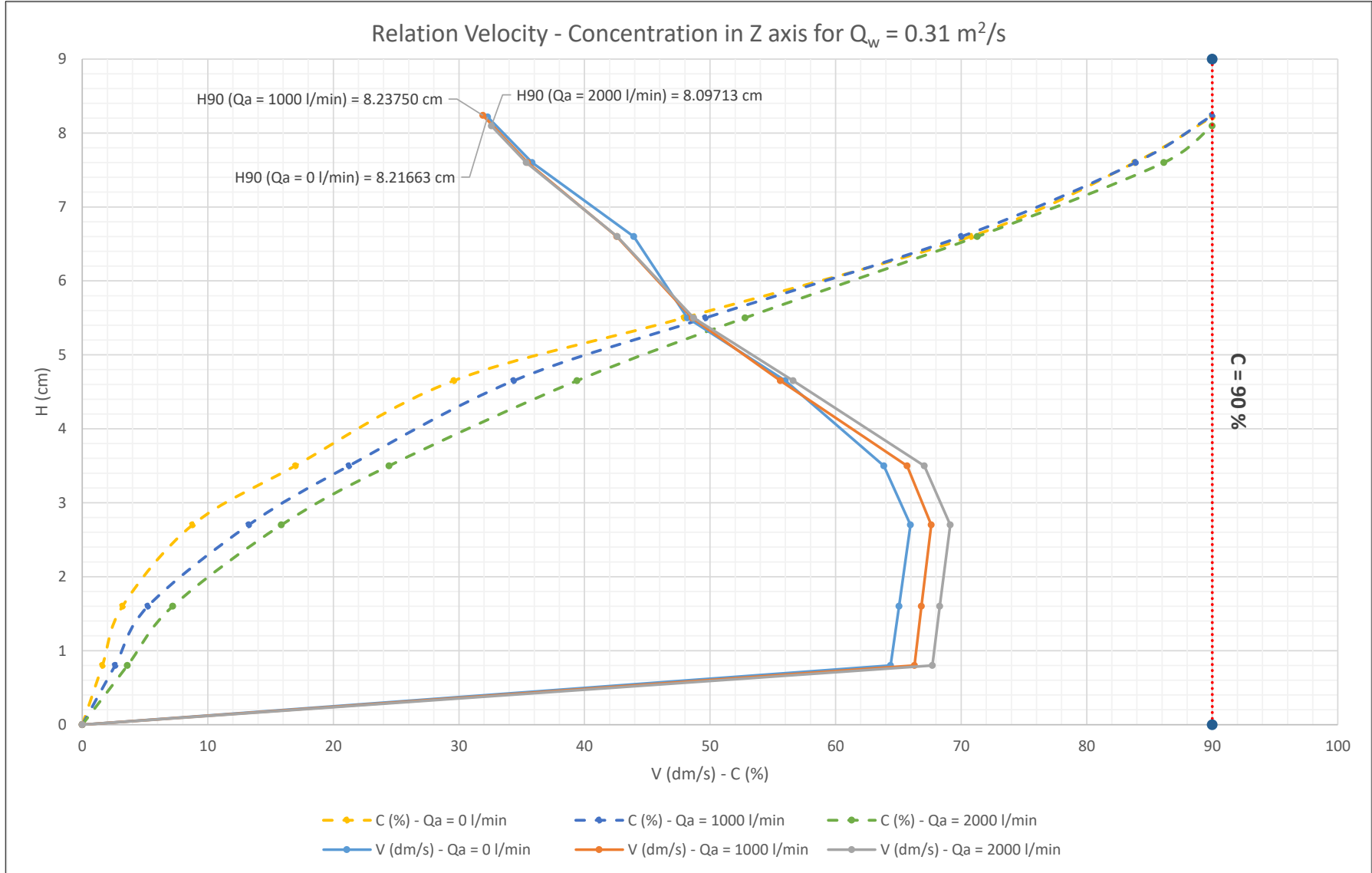


Figure 19. Relation between velocity and concentration profiles of Scenario 1 ($Q_w = 0.31 \text{ m}^2/\text{s}$)

RESULTS AT CHANNEL EXIT SECTION

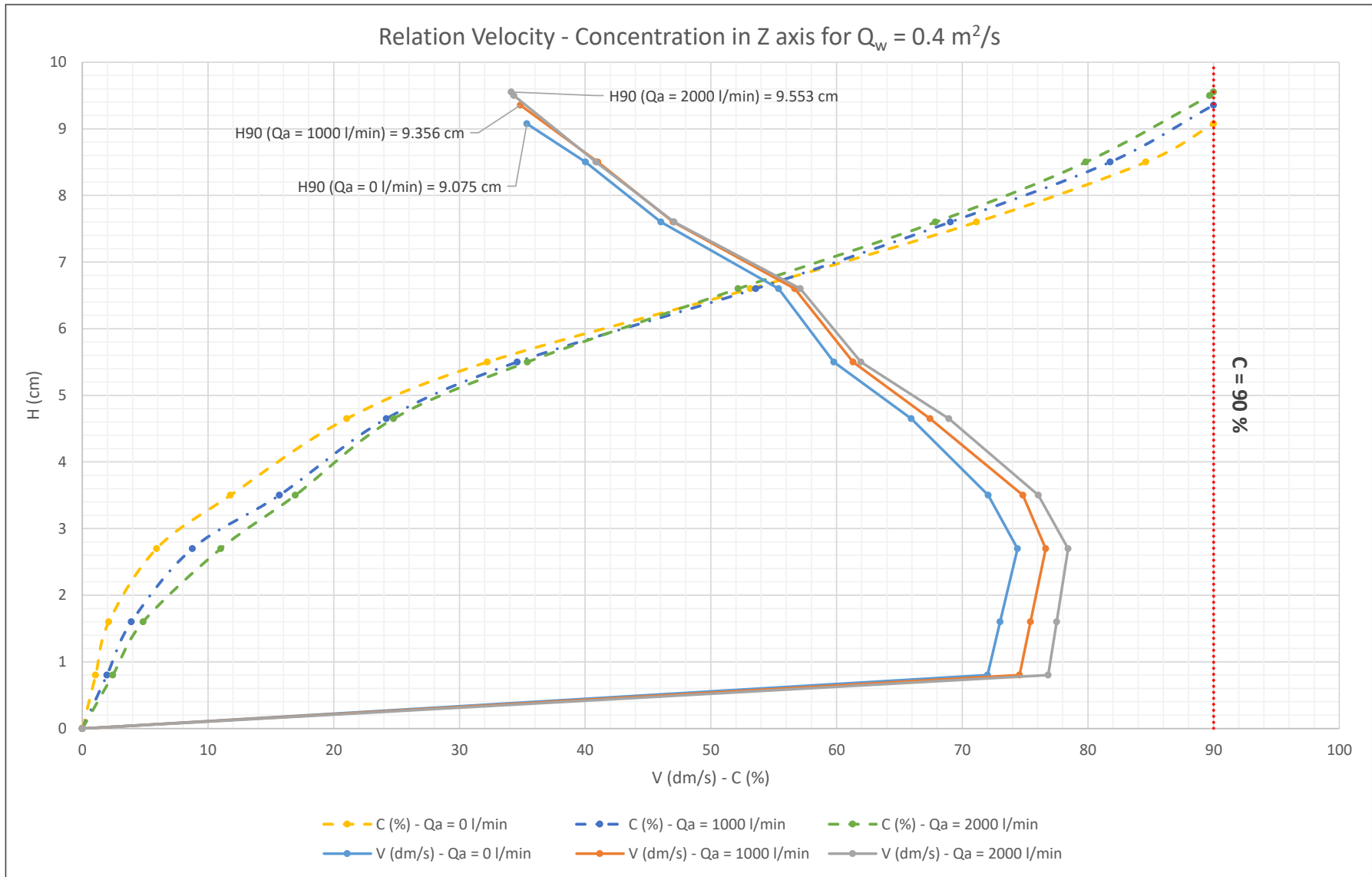


Figure 20. Relation between velocity and concentration profiles of Scenario 2 ($Q_w = 0.4 \text{ m}^2/\text{s}$)

RESULTS AT CHANNEL EXIT SECTION

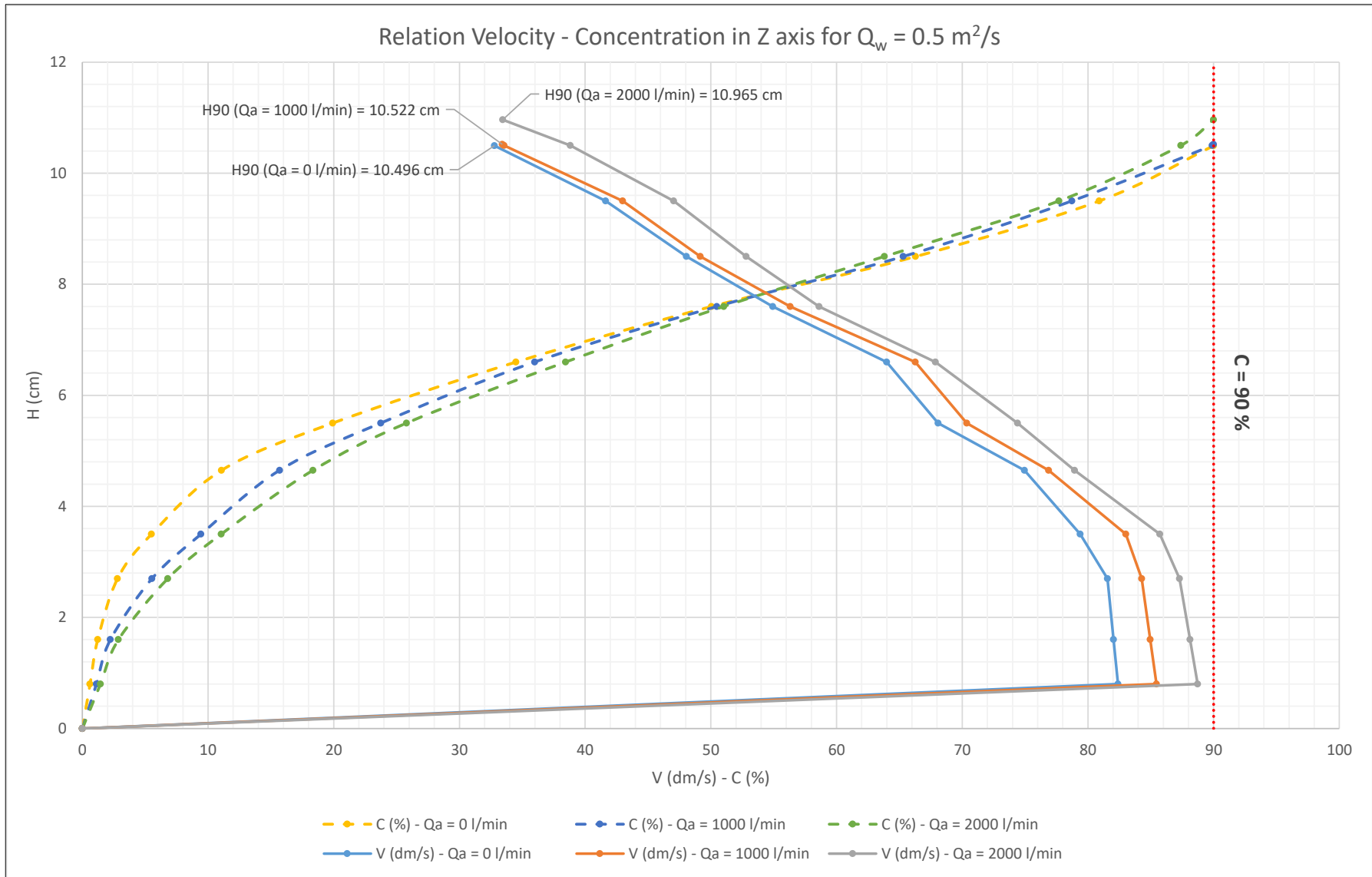


Figure 21. Relation between velocity and concentration profiles of Scenario 3 ($Q_w = 0.5 \text{ m}^2/\text{s}$)

RESULTS AT CHANNEL EXIT SECTION

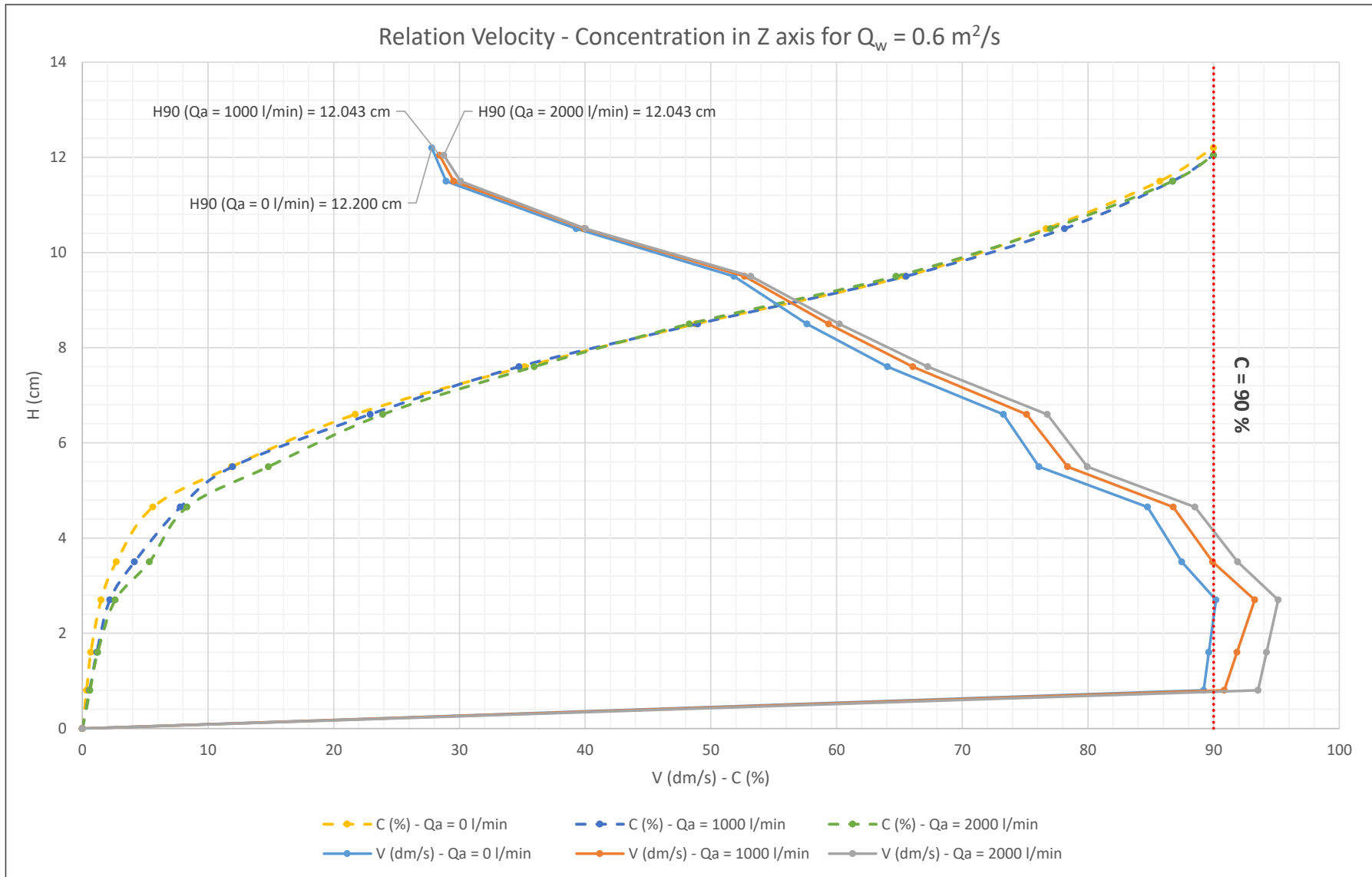


Figure 22. Relation between velocity and concentration profiles of Scenario 4 ($Q_w = 0.6 \text{ m}^2/\text{s}$)

RESULTS ANALYSIS AND DATA

PROCESSING

- Taking velocity and air concentration profiles in the initial and final sections of the channel, it is possible to calculate the average values that characterize spillway flow (V_M , C_M , H_{90M}) and friction slope (I_f) of our test stretch (Table 3)
- Including these data in Manning equation, a representative Manning roughness coefficient (n) is obtained for each scenario (Table 3). Figure 23 relates the Manning roughness coefficient with each concentration (C_M) and demonstrates a roughness reduction with an air concentration increase
- Figure 24, also included in Table 3, shows the reduction rate in % (Δn) of Manning coefficient respect the roughness without aeration

Scenario	V_M (m/s)	C_M (%)	H_{90M} (cm)	n	Δn (%)
1.1	4.5312	14.6396	8.1083	0.0199	9.8119
1.2	4.7725	20.6387	8.1187	0.01919	13.0232
1.3	5.0466	25.6299	8.0485	0.0183	17.0461
2.1	5.4407	13.5246	8.5375	0.01725	5.06
2.2	5.7145	18.9007	8.6777	0.01686	7.1881
2.3	5.9687	22.8966	8.7762	0.01661	8.5816
3.1	6.2831	11.9512	9.2478	0.01628	5.5774
3.2	6.6181	16.3419	9.261	0.01571	8.8573
3.3	6.9457	20.5823	9.4826	0.01547	10.2429
4.1	7.0469	11.0778	10.1002	0.01615	7.857
4.2	7.4091	14.3815	10.0216	0.0156	10.9981
4.3	7.7384	17.4734	10.0217	0.01534	12.5198

Table 3. Average velocity, concentration, H_{90} , n value and Δn at the middle section of channel

DISCUSSION

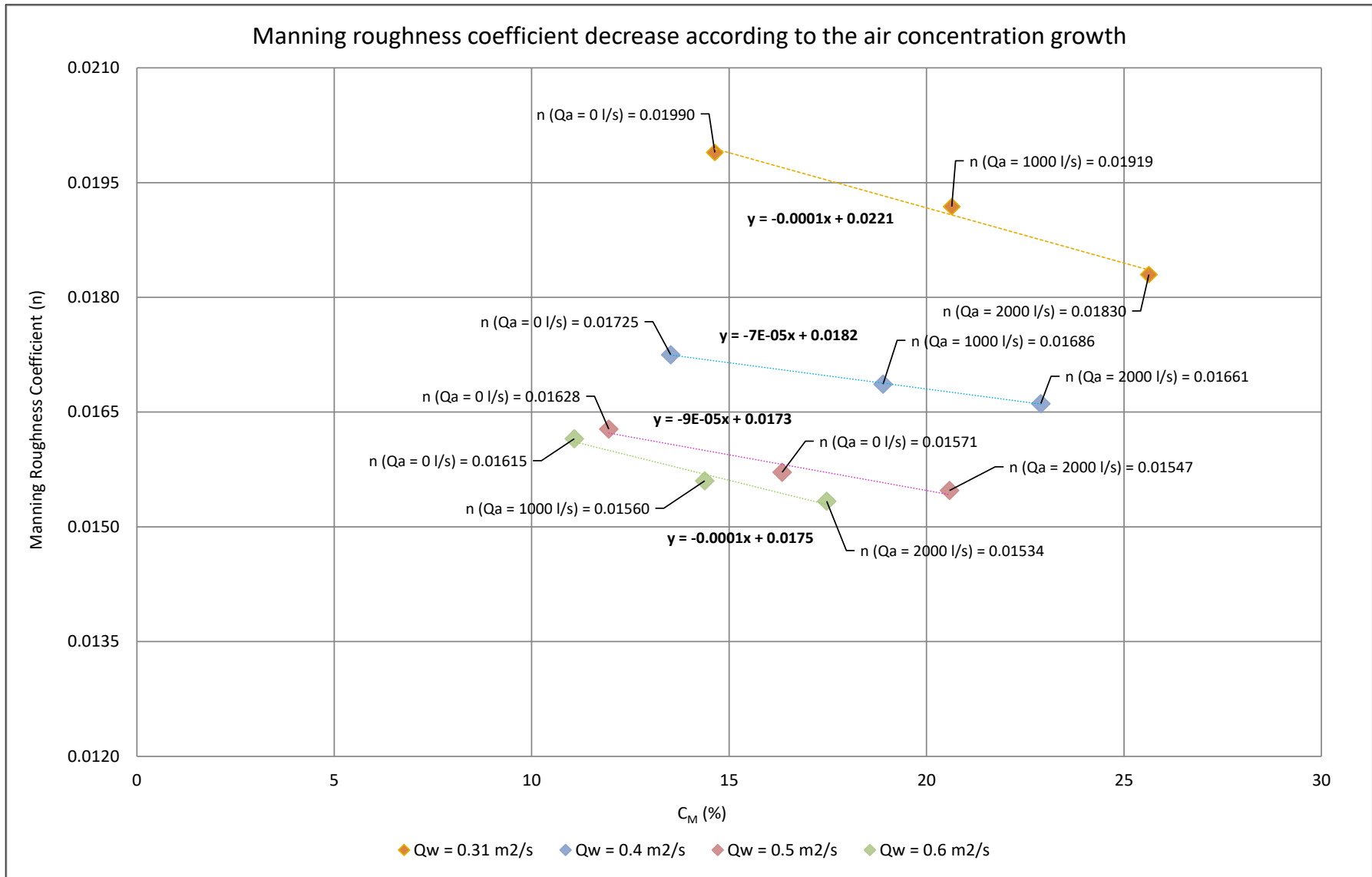


Figure 23. Relation between Manning roughness coefficient (n) and average air concentration (C_M) for all scenarios.

DISCUSSION

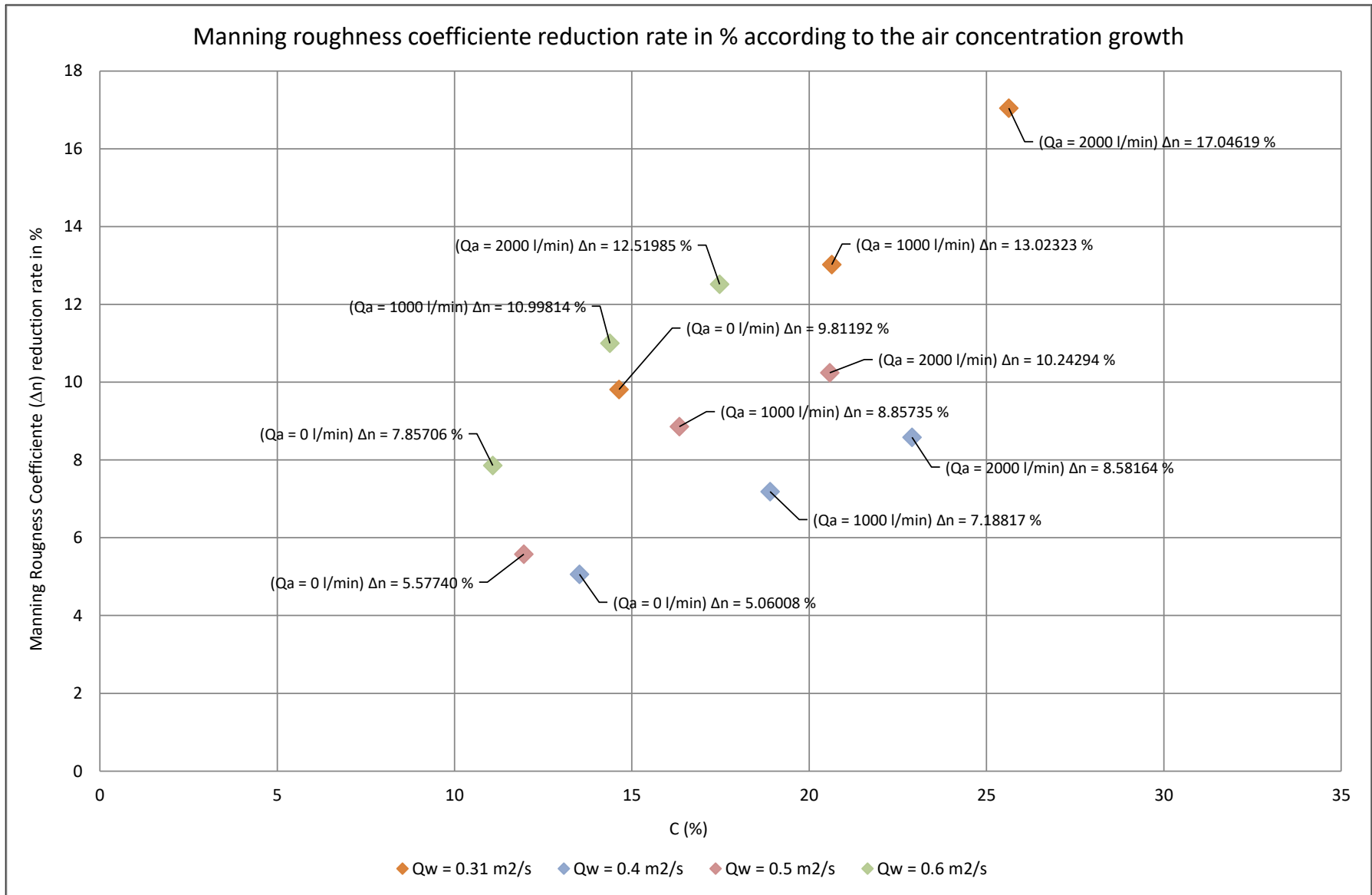


Figure 24. Relation between Manning roughness coefficient reduction rate (Δn) and average air concentration (C_M) for all scenarios.

FUTURE ACTIVITIES AND RESEARCH GUIDELINES

- Next activities will be focused to analyzed the aeration effects over the hydraulic jump
- Intake conditions of still basin are similar to results obtained in the exit section channel (Figure 25)
- Laboratory capacities to determine the flow variables of the hydraulic jump → Evolution of water level and velocity profiles with different concentration intakes (Figure 26 and 27)



Figure 25. Initial condition at intake section of still basin



Figure 26. ADV probe velocity test in hydraulic jump

FUTURE ACTIVITIES AND RESEARCH GUIDELINES

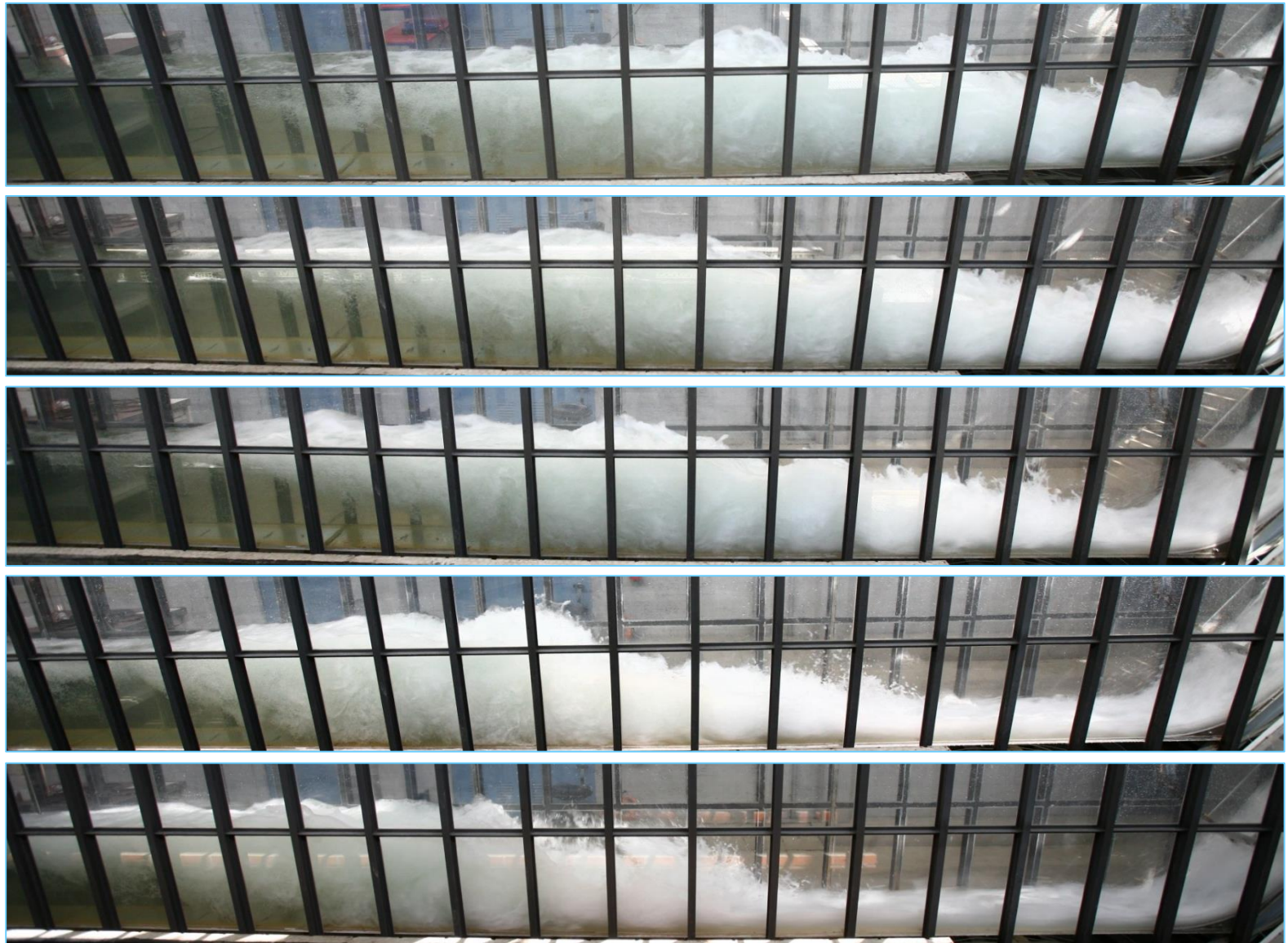


Figure 27. Hydraulic jump evolution with same water rate and different concentration flows

CONCLUSIONS

- Results obtained during the tests show that aeration plays a main role in energy dissipation in open channel flows with supercritical and fully turbulent conditions. With the same water rate, higher air concentration involves lower friction head losses
- Reduction has been quantified by means of the Manning roughness coefficient (n)
- An objective of the global analysis is to propose a correction of Manning equation for aerated and supercritical flows in spillways channels
- Other conclusion seem during the testing process has been the aeration effects over the hydraulic jump. Under same water flow rate, hydraulic jump length decreases with higher air concentration of the still basin intake flow
- This effect is a qualitative appreciation. The phenomena analysis to quantify the hydraulic jump variables will be attached in future lines research

THANKS FOR YOUR ATTENTION

REFERENCE CONTACTS

Juan José Rebollo ¹ (juan.j.rebollo@cedex.es)

David López ¹ (david.lopez@cedex.es)

Tamara Ramos ¹ (tamara.ramos@cedex.es)

Luis Garrote ² (l.garrote@upm.es)

¹ Centro de Estudios y Experimentación de Obras Públicas (CEDEX) – Hydraulic Laboratory

² Universidad Politécnica de Madrid (UPM)